

Design, Implementation and Evaluation of a Real-Time Remote Photoplethysmography (rPPG) Acquisition System for Non-Invasive Vital Sign Monitoring

Constantino Álvarez Casado^{1*}, Sasan Sharifipour¹, Manuel Lage Cañellas¹,
Nhi Nguyen¹, Le Nguyen¹, Miguel Bordallo López^{1,2}

^{1*}Center for Machine Vision and Signal Analysis (CMVS), University of Oulu, Oulu, Finland.

²VTT Technical Research Centre of Finland, Oulu, Finland.

*Corresponding author(s). E-mail(s): constantino.alvarezcasado@oulu.fi;
Contributing authors: sasan.sharifipour@oulu.fi; manuel.lage@oulu.fi;
thi.tn.nguyen@oulu.fi; le.nguyen@oulu.fi; miguel.bordallo@oulu.fi;

Abstract

The growing integration of smart environments and low-power computing devices, coupled with mass-market sensor technologies, is driving advancements in remote and non-contact physiological monitoring. However, deploying these systems in real-time on resource-constrained platforms introduces significant challenges related to scalability, interoperability, and performance. This paper presents a real-time remote photoplethysmography (rPPG) system optimized for low-power devices, designed to extract physiological signals, such as heart rate (HR), respiratory rate (RR), and oxygen saturation (SpO₂), from facial video streams. The system is built on the Face2PPG pipeline, which processes video frames sequentially for rPPG signal extraction and analysis, while leveraging a multithreaded architecture to manage video capture, real-time processing, network communication, and graphical user interface (GUI) updates concurrently. This design ensures continuous, reliable operation at 30 frames per second (fps), with adaptive feedback through a collaborative user interface to guide optimal signal capture conditions. The network interface includes both an HTTP server for continuous video streaming and a RESTful API for on-demand vital sign retrieval. To ensure accurate performance despite the limitations of low-power devices, we use a hybrid programming model combining Functional Reactive Programming (FRP) and the Actor Model, allowing event-driven processing and efficient task parallelization. The system is evaluated under real-time constraints, demonstrating robustness while minimizing computational overhead. Our work addresses key challenges in real-time biosignal monitoring, offering practical solutions for optimizing performance in modern healthcare and human-computer interaction applications.

Keywords: Real-time, Remote photoplethysmography (rPPG), Non-contact biosignal monitoring, Low-power devices, Multithreading, Telemedicine

1 Introduction

The ongoing digital transformation in healthcare and well-being is reshaping care pathways [1][2], introducing new challenges and opportunities, particularly in remote healthcare monitoring and telemedicine [3][4]. This transformation is driven by the need for efficient, scalable, and non-invasive methods to monitor patient health outside traditional clinical settings [5]. Telemedicine, which often involves appointments conducted via video-calls, has become increasingly prevalent [3][5]. However, these interactions largely depend on patients' self-reported data and the occasional use of home medical devices, such as pulse oximeters or blood pressure monitors, which patients must know how to operate. This approach is not only limited but also inconsistent in its application and accuracy.

With the growing need for unobtrusive and continuous health monitoring, contactless technologies using cameras or millimeter wave (mmWave) radars are emerging as a promising solution [6][7]. These technologies leverage techniques such as remote photoplethysmography (rPPG) and remote ballistography (rBSG) to measure physiological parameters without direct contact. rPPG, in particular, uses optical sensors and ambient light to detect blood volume changes in the microvascular bed of tissue, allowing for the extraction of vital signs like heart rate (HR), oxygen saturation (SpO2) and respiratory rate (RR). Studies have demonstrated high agreement between rPPG measurements and traditional medical devices under certain conditions, making it a promising method for non-invasive monitoring [8]. Current methods for recovering physiological signals from videos are mainly divided into unsupervised non-learning methods and deep learning approaches [6]. The former use carefully-designed computer vision and signal processing algorithms while the latter provide end-to-end solutions yet they heavily rely on training data.

While rPPG methods are highly potential, there is a significant gap between current research and practical deployment in real world systems [4]. Existing studies primarily focus on maximizing accuracy using well-curated, publicly available datasets, without addressing the real-time implementation challenges [6][9]. These challenges

include computational and resource constraints of low-power embedded systems, as well as communication issues [9]. To bridge this gap, the algorithms need to be optimized for low power consumption, efficient memory usage, and robustness against frame loss. This involves proper scheduling, synchronization, and strategies to handle frame loss and artifacts such as jitter caused by network quality, ensuring the applicability of the system in realistic scenarios [4][9].

To meet the demands of next-generation telemedicine and human-centered health systems, there is a growing need for edge-capable, modular, and transparent systems that support real-time physiological monitoring in unconstrained environments [10]. These systems not only improve usability and accessibility in clinical and home settings, but also form the foundation for emerging hybrid intelligence paradigms, in which artificial systems interpret human physiological and emotional states to support informed, empathetic decision-making [11]. Real-time implementations also serve a critical exploratory role, revealing system-level challenges such as frame drops, latency, and hardware bottlenecks that often go unnoticed in offline evaluation. Addressing these factors during system development can inform more robust algorithm design, encourage practical trade-offs between complexity and responsiveness, and ultimately enable more trustworthy and scalable deployment [12]. Therefore, designing and validating real-time rPPG systems for low-power platforms is not only a step toward technical feasibility, but a prerequisite for integrating physiological sensing into everyday intelligent systems.

In this context, this article proposes the design and implementation of a real-time rPPG system that aims to measure heart rate and other cardiovascular indicators. This system is specifically optimized for embedded devices, incorporating strategies to mitigate artifacts resulting from network and hardware limitations. Our approach includes a multithreaded architecture to handle image capture, processing, and data communication, ensuring stable operation at 30 frames per second. By using both CPU and GPU for parallel processing, we achieve significant performance improvements, enabling the system to function effectively even under constrained conditions. The main contributions are detailed as follows:

- Developing a prototype for extracting rPPG signals from human faces in real-time, using a pipeline architecture for continuous, efficient vital sign monitoring.
- Optimizing the rPPG system for low-power devices with algorithms designed to minimize power consumption and memory usage, ensuring robust real-time performance.
- Conducting comprehensive speed and accuracy assessments using four datasets, demonstrating the system’s effectiveness and reliability in real-world scenarios for telemedicine and remote health monitoring.

This work addresses the practical challenges of deploying rPPG technology in realistic scenarios, providing a scalable and efficient solution for continuous, non-invasive health monitoring. Our findings offer valuable insights for future digital healthcare systems, supporting the broader adoption of telemedicine and remote monitoring technologies.

2 Related work

The implementation of real-time rPPG systems poses multiple challenges, especially when deployed on low-power embedded devices. These challenges can be broadly categorized into intrinsic issues related to the technology itself and extrinsic factors that arise due to the operational environment conditions [9].

Camera-based systems, such as those used in rPPG systems, often face challenges related to variations in motion and noise [6], ambient lighting changes and low-light conditions [13], occlusions [9], camera distance and resolution [14], and skin tone [15][16]. These challenges are particularly pronounced when these systems are deployed in real-world settings, beyond the controlled conditions of a laboratory, and can severely affect the accuracy and quality of the extracted biosignals [6][9]. These variables can introduce noise and artifacts into the captured data, complicating signal processing and reducing the accuracy of DL-based solutions, making reliable vital sign measurement more difficult. Nguyen et al. (2024) emphasize that effective handling of such artifacts is crucial to improve the resilience of rPPG systems under diverse operational conditions [9].

Beyond the intrinsic challenges of rPPG methodologies and video signal extraction, various external factors can significantly impact the performance of real-time rPPG systems in practical settings. While these systems may perform optimally in controlled laboratory environments, real-world conditions introduce complexities that can compromise their effectiveness. Factors such as sensor limitations [9], network artifacts and limitations [17], and the processing capabilities of embedded devices [18] are critical during deployment. However, their influence is often underestimated in research. Few studies have thoroughly examined these aspects, which are crucial in designing and implementing real-time rPPG methods. This oversight is particularly significant in video streaming for real-time vital sign monitoring, where maintaining signal quality with low latency and limited bandwidth is essential. Despite advancements in 5G and 6G technologies, suboptimal network conditions can still occur, impacting rPPG performance. Techniques such as robust collaborative-relay beamforming can help mitigate video artifacts and network constraints, ensuring reliable real-time vital sign monitoring on wireless devices like smartphones and laptops [19]. Nevertheless, external factors such as network and hardware limitations must be accounted for, as they can significantly affect the performance of rPPG systems. Issues such as video codecs and video compression [20], video resolution [9][14], frame rate variations [9][21], and network jittering and frame loss due to network instability [9] can disrupt the continuity and integrity of data, essential for smooth biosignals extraction and analysis. Video compression can introduce noise and spatio-temporal artifacts into the biosignals [22][23]. Similarly, variations in frame rate and resolution can alter the morphology and frequency features of the extracted signals, impacting the accuracy of physiological signal extraction [9]. Research has also shown the importance of choosing the best image format to extract biosignals with better SNR and quality [24].

These factors should be considered during the design phase to avoid unexpected performance issues in real-world applications. Optimizing systems that perform well under lab conditions for real-world deployment often requires compromises, affecting expected performance. Addressing

the above challenges requires not only robust algorithm design but also novel system architectures that can accommodate the demands of real-time processing. Botina-Monsalve et al. (2022) present RTrPPG, an ultra-light 3DCNN model designed to balance accuracy and processing time for real-time applications [24]. This model optimizes the architecture by reducing input image dimensions and using a temporal-frequency-based loss function. These adjustments significantly improve inference speed, achieving 28.6 milliseconds per frame on an Intel Xeon CPU at 2.4 GHz and 2.32 milliseconds on an Nvidia GeForce RTX 2070 GPU. While these improvements make RTrPPG suitable for real-time deployment, it may still face challenges in low-powered embedded systems. Hasan et al. (2022) adapted the deep learning models for resource-constrained devices leveraging pruning and quantization techniques [25]. Their approach reduced the model size, power consumption, memory usage, and latency to deploy the rPPG systems on edge platforms, including NVIDIA Jetson Nano, Google Coral Development Board, and Raspberry Pi.

Furthermore, the development of specialized hardware accelerators and optimized neural network architectures contributes to enhancing the feasibility of deploying advanced computer vision and signal processing techniques on low-power devices [26]. These accelerators, including AI-specific units, enhance performance and efficiency, making advanced techniques more feasible in constrained environments. Examples include the Sagitta accelerator [27], which is designed for specific deep learning architectures and improves energy efficiency and reduces latency. AI accelerators like the Neural Processing Unit (NPU) in the Qualcomm Snapdragon 855, the Intel Myriad X Visual Processing Unit (VPU), and the Nvidia Jetson Nano with its Maxwell architecture offer substantial computational power beyond standard GPUs [28], especially for DL-powered systems. Open-source frameworks such as OpenVINO, ExecuTorch from PyTorch, ONNX Runtime (ORT), and AMD RyzenAI optimize and accelerate model inference on these specialized hardware platforms. However, not all end-users have access to these accelerators, and integrating them can be complex and costly [28]. While beneficial for DL models, these accelerators offer limited

advantages for traditional computer vision or signal processing tasks. Reliance on specific hardware can also limit portability and flexibility across different platforms. General-purpose frameworks like OpenCL, OpenMP, OpenACC, or OpenGL leverage the computing power of available hardware in embedded devices. These frameworks provide a versatile environment for parallel processing tasks [29], improving performance for a wide range of applications. The advantage of using OpenCL and OpenGL is their broad compatibility with various hardware, which enhances portability [29]. However, these frameworks may not offer the same level of optimization for DL-based tasks as specialized AI accelerators. Considering these factors during design ensures practical and effective solutions for diverse deployment scenarios.

Effective real-time systems require well-structured software architectures and precise concurrency control mechanisms [30]. To achieve optimal performance and responsiveness, researchers and practitioners have explored the potential of multithreading and multiprocessing [31–33]. Buttazzo (2011) emphasizes the critical role of predictable scheduling algorithms in ensuring timely task execution within constrained resource environments [34]. These algorithms can be implemented at multiple levels, including hardware, low-level software, and the application layer [32]. Predictable scheduling can be implemented within the application itself, especially in real-time stream-processing applications that involve multiple subtasks needing coordination. This approach is essential for ensuring tasks execute within strict time constraints, managing task assignment to system resources like CPU cores to guarantee completion within predictable limits [34]. Key features of predictable scheduling include determinism, which ensures that system behavior can be precisely predicted, timeliness, which guarantees that tasks meet their deadlines to avoid critical failures, and efficiency, which optimizes resource use to prevent idleness and enhance throughput. Lorenzon et al. (2015) highlight the benefits of multithreading in improving system performance, particularly on devices with limited computational resources, such as embedded systems [35]. Task parallelism involves breaking down complex tasks into smaller, independent subtasks

that run concurrently, improving system throughput by using multiple cores [32, 36]. It includes decomposition (dividing tasks into subtasks), concurrency (executing subtasks independently), and asynchronicity (tasks proceed without waiting for others). Other important models include data parallelism, which distributes data across processors, thread-level parallelism, which uses multiple threads within a core, fork-join parallelism, which splits tasks into parallel threads and rejoins them, and hybrid parallelism, which combines task and data parallelism [32]. To coordinate concurrent activities effectively, event-driven synchronization at the application level is crucial [37]. This involves a main thread managing an event loop that interacts with other threads, handling task dependencies, and preventing performance bottlenecks. This method enhances system responsiveness by avoiding blocking operations and ensuring efficient resource use. Synchronization primitives like mutexes are essential for protecting shared resources from concurrent access. By enforcing mutual exclusion, mutexes prevent race conditions and data corruption. However, blocking mutexes can cause performance issues due to thread waiting. Non-blocking alternatives, such as spinlocks or optimistic concurrency control, offer more efficient solutions in specific scenarios [35]. The evolution of programming languages has significantly impacted the development of concurrent applications. Traditionally, low-level synchronization primitives, such as semaphores and condition variables, were primarily available through operating system APIs. However, modern languages increasingly incorporate higher-level concurrency constructs, such as promises/futures (e.g., C++11, Python, ECMAScript 7), monitors (e.g., Ada 95, Java), and parallel programming models like fork-join (e.g., OpenMP) and work stealing (e.g., Intel’s TBB, Apple’s GCD). These advancements simplify concurrent programming and enable developers to harness the power of multi-core processors more effectively [31, 38].

Building on existing research, we have designed a real-time rPPG system based on a modular pipeline architecture, allowing easier optimization and parallelization. We optimized each pipeline block at both the algorithm and data levels. This included selecting algorithms with reduced computational complexity, implementing approximate methods where full precision was unnecessary,

and choosing algorithms amenable to parallel processing. We incorporated pruning strategies to limit unnecessary computations and applied memoization by caching intermediate results to accelerate subsequent operations. Memory management was improved through the use of memory pooling and precise data alignment, which kept shared data structures persistent throughout execution, thus minimizing the overhead from frequent memory allocation and deallocation. Furthermore, we utilized data parallelism to effectively distribute processing tasks across multiple CPU cores, thereby improving overall performance and reducing latency. Additionally, we integrated real-time quality metrics to evaluate the input data, specifically estimating factors such as face movement. This approach ensures that only high-quality data is processed, thereby improving efficiency and speed by avoiding unnecessary computations on low-quality inputs. We implemented multithreading and task-parallel techniques using C++14, employing threads and mutexes to prevent data races. Asynchronous threads were utilized to operate independently, keeping the main processing flow unblocked and enhancing system responsiveness. This setup ensures the camera thread always provides the latest frame, eliminating the need for intentional frame-dropping strategies and maintaining consistent real-time performance. A central master thread maintains a regular frame rate and orchestrates the system. The design leverages multi-core and heterogeneous architectures, allowing tasks to run on dedicated CPU cores or with GPU support, and supports distributed processing. An event-driven graphical user interface (GUI) efficiently uses hardware resources, with the master thread generating events at regular intervals for continuous data capture and processing. These strategies improve performance and responsiveness, making the system suitable for real-time rPPG applications on low-power devices. The following sections detail our rPPG pipeline and real-time architecture design, highlighting implementation details and benefits.

3 Remote photoplethysmography pipeline

To extract rPPG signals from face videos, we use the unsupervised, non-learning-based Face2PPG pipeline [6]. It integrates computer vision and signal processing techniques to deliver precise and reliable rPPG signal extraction, making it suitable for various applications in health monitoring and biometric analysis. The pipeline begins with face detection and alignment, using either DL models or traditional ML methods. Subsequently, skin segmentation isolates regions of interest (ROIs) in the facial region for signal extraction. Dynamic ROI selection is used to identify areas with optimal signal quality while discarding regions with occlusion, low contrast, or potentially poor signals. The pipeline then extracts raw rPPG signals from the selected ROIs. These signals undergo filtering to remove noise, enhance quality, and isolate the frequency bands of interest. Following this, the RGB signals are transformed into physiological signals (PPG signals), and spectral analysis is performed to derive physiological parameters. Post-processing steps compute vital signs such as heart rate (HR), respiratory rate (RR), blood oxygen saturation (SpO2), and heart rate variability (HRV). Additionally, the pipeline incorporates movement and facial expression stabilization through geometric normalization using facial landmarks. This stabilization maintains consistency in ROI selection despite facial movements and expressions, ensuring robust and accurate signal extraction across several state-of-the-art datasets [6].

The adaptation of the Face2PPG pipeline for real-time operation, as detailed in the subsequent subsections, followed a systematic and iterative refinement process. Each module was critically analyzed and optimized to balance computational efficiency, essential for low-power devices, with the signal fidelity required for reliable physiological measurement. This approach was informed by the practical challenges inherent in live video processing and real-time constraints, as highlighted by research trends in embedded systems [12].

3.1 Adapting and optimizing the Face2PPG pipeline to real-time operation

The proposed real-time prototype was developed using C++ (C++14 standard) due to its performance and ability to manage system complexity. We used several optimized libraries: **OpenCV 4.6.0** for computer vision tasks [39], **Dlib 19.23** for machine learning tasks [40], and **Qt 5.13.0** for developing a cross-platform GUI [41]. These libraries were selected for their functionalities and performance benefits, essential for real-time image processing applications. The adaptation of the Face2PPG pipeline for real-time operation involves the optimization and refining of the following sequential stages and modules:

1. **Face Detection and Tracking:** Our real-time system uses two face detectors, each with unique characteristics. The first, YuNet by Wu et al. [42], is a CNN-based detector known for its compactness and speed, with a size under one megabyte. Using the MobileNet structure [43], YuNet has 85,000 parameters, achieving detection rates of 909 fps for 224x224 (1.1 ms), 625 fps for 320x320 (1.6 ms), and 105 fps for 649x480 (9.5 ms) on an Intel i7-12700K CPU in C++ over 1,000 iterations [42]. YuNet is optimized for real-time applications on CPUs, making it suitable for mobile and embedded devices while maintaining robust performance under varying conditions. The second detector, Dlib [44], uses a method based on Histogram of Oriented Gradients (HOGs) [45]. This approach is effective for CPU use, particularly in detecting frontal and slightly non-frontal faces, and remains reliable even under minor occlusion. To maintain consistent face tracking, faces are detected every three frames, optimizing computational resources and enhancing real-time performance. This method updates a face flag to indicate the presence or absence of a face in the focus area (center rectangle marked in the GUI), allowing for effective tracking even if the face is temporarily obscured or moves out of focus. We use the face detectors as a primary step for applying a face alignment model on the detected faces. By asking users to stay still within the set area, we reduce movement

errors, leading to more accurate estimations of vital signs.

2. **Face Alignment:** In the Face2PPG pipeline, precise facial alignment is crucial for geometric face normalization and accurate skin segmentation, important for extracting reliable physiological signals. This alignment also supports accurate tracking of head movements and facial expression analysis, providing insights into patient well-being. To ensure real-time performance on low-power computing systems, we optimized face alignment models for accuracy, speed, and memory-efficiency. While Deep Alignment Network (DAN) models offer high accuracy, their computational demands make them unsuitable for such environments. Instead, we focused on optimizing and training two fast, non-deep-learning-based models: Ensemble of Regression Trees (ERT) and Local Binary Features (LBF) algorithms. These models deliver rapid and precise face alignment in real-time. Our optimized models significantly outperform existing implementations of these algorithms [46]. Using the ERT algorithm in Dlib, we achieved a speed of up to 530 fps on a CPU, offering a faster and more memory-efficient solution while maintaining high accuracy, even in challenging scenarios [46]. One such challenge is the 'jittering' effect in facial videos, where small fluctuations in landmarks between frames can affect skin segmentation. Fast head movements can further disrupt landmark detection in real-time applications. To address these issues, we enhanced the training process and incorporated temporal information to improve landmark tracking in videos. A key strategy was integrating domain-specific data into training, including images with challenging poses or low-light conditions, annotated using a teacher-student approach, improving model performance under complex conditions [46].

3. **Skin Segmentation and Region of Interest Selection:** The approach uses a novel geometric segmentation method based on facial landmark points [6]. The proposed segmentation method normalizes the face in each frame by mapping triangles from the detected face to a reference shape. This generates a spatiotemporal matrix of normalized faces, ensuring

consistent signal measurement across frames, regardless of pose or movement. Although some landmark variability exists across video frames, it is reduced compared to skin color segmentation methods [46]. We have also developed a deep-learning-based skin segmentation method using an uNET architecture. However, it suffers similar problems, caused by the small number of annotated facial skin masks, resulting in underfitted models [47]. We instead use an Alpha-Beta filter to stabilize the landmarks in each frame and reduce small changes. Regarding ROI selection, we strategically target three specific facial areas: cheeks and forehead. These regions, characterized by a dense network of blood vessels, are optimal for extracting biosignals from the face as demonstrated in [6]. This process facilitates the extraction of raw RGB signals from these areas, preparing them for the next steps.

4. **RGB to BVP Transformation (rPPG):** The real-time system uses the CIE-Lab color space for RGB to BVP transformation. CIE-Lab was selected over methods such as CHROM, OMIT, and POS due to its efficient computation [6] without temporal dependency, allowing for independent conversion of each frame. Additionally, CIE-Lab provides a wider dynamic range than the simplest method (the green channel approach [48]) and effectively isolates the chrominance channel, which is essential for detecting blood-related signals [6]. Rather than converting the entire frame to CIE-Lab format, the system computes the average RGB values within the ROI and converts only these averages to CIE-Lab. This approach reduces the computational cost by performing a single conversion per ROI rather than processing every pixel. The conversion process is detailed as follows:

- (a) **Step 1: RGB to XYZ.** First, the average RGB values are normalized to the range [0, 1]:

$$R_{norm} = \frac{R}{255}, \quad G_{norm} = \frac{G}{255}, \quad B_{norm} = \frac{B}{255} \quad (1)$$

Gamma correction is applied:

$$R_{linear} = \begin{cases} \left(\frac{R_{norm} + 0.055}{1.055} \right)^{2.4}, & \text{if } R_{norm} > \beta \\ \frac{R_{norm}}{12.92}, & \text{if } R_{norm} \leq \beta \end{cases} \quad (2)$$

where $\beta = 0.04045$.

The same correction is applied to G_{linear} and B_{linear} . The linearized RGB values are then converted to XYZ using the following matrix:

$$\begin{pmatrix} X \\ Y \\ Z \end{pmatrix} = \begin{pmatrix} 0.4124 & 0.3576 & 0.1805 \\ 0.2126 & 0.7152 & 0.0722 \\ 0.0193 & 0.1192 & 0.9503 \end{pmatrix} \begin{pmatrix} R_{linear} \\ G_{linear} \\ B_{linear} \end{pmatrix} \quad (3)$$

- (b) **Step 2: XYZ to CIE-Lab.** The XYZ values are normalized relative to the reference white point (D65: $X_n = 95.047$, $Y_n = 100.000$, $Z_n = 108.883$):

$$X' = \frac{X}{X_n}, \quad Y' = \frac{Y}{Y_n}, \quad Z' = \frac{Z}{Z_n} \quad (4)$$

Each normalized value is transformed as follows:

$$f(v) = \begin{cases} v^{1/3}, & \text{if } v > 0.008856 \\ 7.787v + \frac{4}{29}, & \text{if } v \leq 0.008856 \end{cases} \quad (5)$$

Finally, the CIE-Lab values are computed:

$$L^* = 116 \cdot f(Y') - 16 \quad (6)$$

$$a^* = 500 \cdot [f(X') - f(Y')] \quad (7)$$

$$b^* = 200 \cdot [f(Y') - f(Z')] \quad (8)$$

This optimized conversion method minimizes computational overhead while effectively targeting the chrominance channel, which is important for accurately extracting blood-related signals.

5. **Buffering and Windowing:** The system maintains a buffer implemented with a C++ *deque* that holds up to 360 samples of the a-channel values from the CIE-Lab color space, corresponding to a 12-second window. This buffer supports the real-time computation of HR and RR by continuously updating with the most recent data. The buffer functions in a rolling manner, where each new sample is added to the back (*push_back()*) and the oldest sample is removed from the front (*pop_front()*), ensuring no data is lost and calculations are always based on the latest available data. Once 90 samples (3 seconds) are collected, the system computes the first HR value and updates

it every second as new data arrives. After 8 seconds (240 samples) of uninterrupted data, the system marks the signal as stable, indicating that the data is reliable for further processing and transmission. The first RR value is calculated once the stability condition is met, ensuring that the RR computation is based on a sufficiently long and stable segment of data. Once the signal is stable, the system shifts to using continuous 12-second windows (360 samples) for frequency analysis, ensuring more accurate HR and RR extraction. The buffer size and window duration are configured to optimize real-time performance while minimizing computational overhead. The stability flag ensures that only uninterrupted and reliable data is used for post-processing and biosignal transmission, enhancing the overall accuracy and robustness of the system.

6. **Dynamic Signal Filtering:** Signal filtering is essential for isolating frequency components and reducing noise in physiological signals for improved HR and RR measurements. The system uses a 61-tap Finite Impulse Response (FIR) filter with a linear phase design, which preserves the temporal structure of the signals and avoids phase distortion. The filter is tailored for specific physiological ranges. For HR, a band-pass filter (BPF) is applied within a range of 0.75 to 4.00 Hz (45 to 240 bpm), with a narrower range for real-time display (0.8 to 2.0 Hz, 48 to 120 bpm). For RR, a low-pass filter (LPF) is set at 0.7 Hz, covering up to 42 breaths per minute.

The 61 taps in the BPF offer a balance between frequency selectivity and computational cost. More taps would sharpen the filter response but increase the processing load, while fewer taps would reduce filtering performance.

The filter coefficients are calculated using the sinc function to design the band-pass filter:

$$m = n - \frac{N-1}{2}, \quad \text{for each } n \quad (9)$$

$$h[n] = \begin{cases} \frac{\phi - \lambda}{\pi}, & \text{if } m = 0, \\ \frac{\sin(m \cdot \phi) - \sin(m \cdot \lambda)}{\pi \cdot m}, & \text{if } m \neq 0. \end{cases} \quad (10)$$

where N is the total number of filter taps, n is the index of the filter tap ranging from 0 to $N - 1$, and m is the index relative to the center of the filter. ϕ and λ are the angular frequencies corresponding to the upper and lower cutoff frequencies, respectively. The value of $h[n]$ represents the filter coefficient for the n -th tap of the filter.

By storing past values of the input signal in a shift register, the filter maintains continuity across consecutive data windows. This minimizes transient effects that can occur at the beginning of each new window, ensuring smoother and more consistent filtering. The fixed filter coefficients were selected to ensure efficient and reliable signal extraction, while the buffering of past data reduces artifacts without adding significant computational overhead.

7. **Frequency Analysis:** The system performs frequency analysis on heart and respiratory signals using the Discrete Fourier Transform (DFT). A Hamming window is applied to reduce spectral leakage, and zero-padding is used to improve frequency resolution. The Power Spectral Density (PSD) is computed from the DFT output by summing the squared magnitudes of the real and imaginary components of each frequency bin. To ensure accurate frequency analysis despite frame rate variations, the system recalculates the frame rate every second based on captured timestamps. The HR is determined from the dominant frequency in the PSD, within the range of 0.75 to 2.5 Hz (45 to 150 bpm), after filtering out noise outside this range. The system refines HR estimation iteratively by excluding erroneous peaks and outliers. Once the signal is stable, frequency analysis continues using a 12-second sliding window for more robust HR and RR calculations. For increased robustness, Welch’s method is optionally applied in cases where the signal may exhibit noise or instability due to motion artifacts or minor inconsistencies in the signal capture process. By dividing the signal into overlapping segments and averaging their periodograms, Welch’s method reduces spectral variance, providing more stable HR and RR estimates in challenging scenarios. Although this method requires additional computational

resources, it improves the reliability of the frequency analysis when the signal is less stable or contains transient disturbances.

4 Real-time system architecture design and implementation

To integrate the Face2PPG rPPG extraction pipeline into a remote biosignal acquisition system, as detailed in [49], a real-time prototype application was designed and developed. This application is engineered to extract non-contact-based PPG signals remotely or in-situ from human faces using video streams (e.g., videocalls), enabling the calculation of vital signs essential, for instance, in primary healthcare assessments. The architecture follows a modular pipeline design, where the core rPPG system operates sequentially, with each component performing a specific task in sequence, relying on the output of the previous stage. This structured approach is designed for efficiency in a real-time context and is depicted in Figure 1. The architecture was incrementally developed through iterative implementation and testing, guided by practical constraints observed during real-time operation such as frame drops, responsiveness issues, and task synchronization challenges. These insights informed the modular design and scheduling strategy, ensuring that each component could operate efficiently and independently while maintaining the performance required for accurate physiological signal estimation under realistic deployment conditions [50].

The system architecture is organized into four primary functional blocks: the collaborative UI, video capture, real-time processing and analysis, and the network interface, as shown in Figure 2. These blocks provide the necessary infrastructure for data handling, user interaction, and network communication, while the core of the system, the optimized Face2PPG pipeline, handles the rPPG signal acquisition and analysis, allowing for the extraction of physiological signals from video data. The collaborative UI plays a key role in ensuring optimal conditions for rPPG signal extraction. It provides real-time video quality metrics and user feedback, helping to maintain consistent biosignal

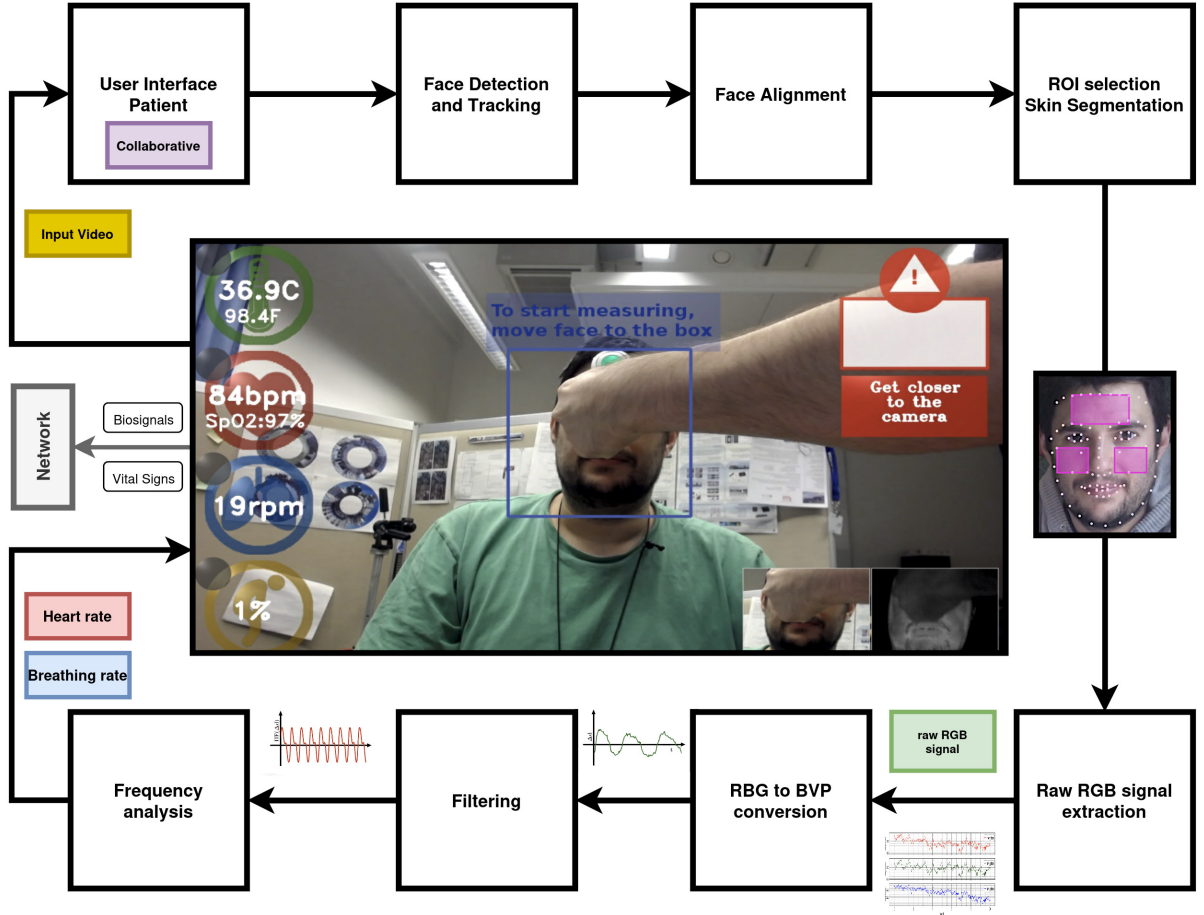


Fig. 1: Architecture overview of the proposed real-time rPPG application, comprised of several interconnected components, each executing a specific task.

capture by guiding the user on appropriate positioning and environmental factors such as lighting. The video capture thread is dedicated to continuously acquiring frames from the camera. Each frame provides a sample for the rPPG analysis pipeline, and it is critical to avoid frame dropping to maintain regular sampling of the biosignal. This thread minimizes delays and compensates for camera jitter, ensuring consistent frame capture for precise signal analysis. The real-time processing and analysis block is the optimized implementation of the Face2PPG pipeline. This block operates concurrently with the other blocks and performs critical tasks such as face detection, alignment, and face normalization. The processed video data is then analyzed to extract physiological signals in real time, using optimized algorithms to support immediate and accurate analysis. The

network interface operates with three different threads: two threads handle continuous video streaming via HTTP, and a third thread manages the RESTful API. The video streams include the main camera feed (cropped to the face) and a normalized pulsating face stream, both transmitted as MJPEG. The RESTful API thread responds to GET requests, providing the latest computed vital signs, including HR, RR, and oxygen saturation (SpO2). In parallel, the GUI thread continuously updates the user interface with the latest video frames and vital sign values. This ensures that the interface remains responsive and up-to-date without impacting the core data processing or network transmission tasks. By distributing these tasks across multiple threads, the system leverages multicore processors to maintain high performance and reliability. The multithreaded design allows

for concurrent execution of tasks, ensuring real-time biosignal monitoring and analysis without introducing bottlenecks or latency, while supporting continuous user feedback and data streaming.

4.1 Reactive-based programming design

The application implements a reactive programming model that combines aspects of Functional Reactive Programming (FRP) and the Actor Model, making it well-suited for real-time interactive systems that require rapid responses and efficient resource management. The event-driven design of the system is central to its operation, with key computational tasks triggered dynamically by events such as face detection. This approach reflects the principles of FRP, where operations are executed only when specific conditions are met, ensuring efficient use of computational resources. Although the core pipeline is modular and sequential, its event-driven nature resembles dataflow programming, a concept related to FRP. The system reacts to inputs (such as the appearance or absence of a face) by activating the necessary processing tasks as shown in Figure 1. At the same time, regular updates are maintained through a timer-driven mechanism that coordinates the activities of the system components. The asynchronous architecture follows the Actor Model, with independent threads handling specific tasks such as video capture, processing, GUI, and network operations. These threads run concurrently and are managed by a central event loop. When possible, threads are distributed across multiple cores of the processor, enhancing parallelism. The main thread synchronizes system operations by aggregating updates from these threads at regular intervals. This design ensures that no thread blocks another or causes unnecessary waiting, even when data exchange between threads is required. As a result, the system maintains continuous, efficient operation without interruption. This hybrid model blends the declarative nature of FRP with the concurrent, message-passing framework of the Actor Model. By combining these programming paradigms, the system achieves robust real-time performance, handling both event-triggered reactions and continuous updates seamlessly within a multithreaded, multi-core environment.

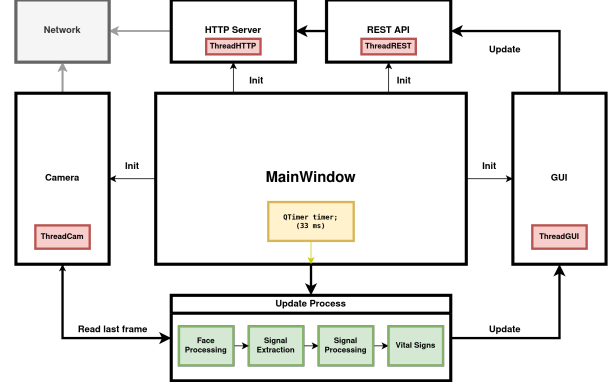


Fig. 2: Implementation design of the proposed real-time rPPG application.

The system is coordinated by a central process called **MainWindow**, which manages timing and controls the execution of pipeline processes, as shown in Figure 2. The *MainWindow* initializes system components like the camera component and GUI, while also managing operational data such as the frame counter, biosignal values, and timestamps. To maintain a consistent frame rate of 30 frames per second, the *MainWindow* uses the **QTimer** class from the Qt framework to trigger the main loop every 33 milliseconds. The *QTimer* emits a `timeout()` signal at regular intervals, which activates the main loop to process frames, update the GUI, and manage other real-time tasks. In a multithreaded environment, *MainWindow* interacts with other threads handling image capture, face detection, and signal processing through their event loops. This design keeps real-time performance steady while minimizing system overhead. By placing components in separate threads, the system avoids blocking the main thread during camera and GUI operations. This design ensures that image capture and GUI updates occur concurrently with other processing tasks, maintaining smooth, uninterrupted operation. The *UpdateProcessFrame* function in the *MainWindow* process manages real-time processing and interface updates. It is triggered every 33 milliseconds by the frame in *MainWindow* to maintain a consistent frame rate of 30 frames per second. The function retrieves the last available frame from the camera thread and calls the *detectFacesRGB* method from the *Process* class

to detect faces and extract biosignals. After processing, the function updates the *DataContainer* with the relevant data, including RGB frames, frame number, facial landmarks, face activity status, and calculated vital signs. A global timer tracks processing time, and the frame counter records the number of frames processed. If a face is not detected in the current frame, a counter is incremented. The system initiates a reset after 60 consecutive missed detections. Once processing is complete, the *newRGBframe* flag is reset to indicate that the current frame has been fully processed and the system is ready to receive the next frame for further processing. Finally, the *UpdateProcessFrame* function provides the latest data, which is then used by the *MainWindow* to update the GUI and increment the frame counter. The GUI runs in a separate thread, continuously rendering the processed data for real-time display. Simultaneously, to support real-time monitoring and integration with other applications, the system includes a RESTful API and an HTTP server, both operating in their own thread. This API exposes an endpoint that accepts HTTP requests, allowing external clients to retrieve the most recent frame and computed HR, SpO2, and RR values. Upon receiving a request, the service accesses the latest data from the *DataContainer* and responds with the current frame and vital sign values in a structured format.

This multithreaded design allows the system to handle incoming network requests, transmit real-time data, and update the GUI concurrently without interference with the main processing tasks. The modular and thread-based architecture ensures that camera and GUI operations, along with network services, operate smoothly and without interruptions, demonstrating the system's real-time processing capabilities. Efficient computational algorithms, optimized for hardware constraints, enable continuous biosignal extraction and vital sign calculation while ensuring effective resource management through multiprocessing and parallelization.

4.2 Real-time implementation of the network software components

Following the real-time architecture described earlier, the network components are designed to run

concurrently with other system processes, ensuring consistent data transmission and integration with external applications.

The RESTful API is initialized in the *MainWindow* constructor, where a dedicated thread is created to run the *initializeREST* function. This function configures the REST service using the *Restbed* library¹, which handles HTTP requests asynchronously within the dedicated thread. The service operates on port 8080, and the resource endpoint */vhealth* is used to provide vital sign data. When a client makes a request to <http://127.0.10.1:8080/vhealth>, the system responds with seven formatted values as follows:

```
%05.1f,%05.1f,%05.1f,%d,%d,%08.1f,%08.1f
```

These values correspond to the following variables:

- **g_hr**: Heart Rate
- **g_br**: Breathing Rate
- **g_O2**: Oxygen Saturation (SpO2)
- **g_seeuser**: Indicator of whether a user is present
- **g_stable**: Indicator of whether the values are considered reliable
- **g_hr_graph**: Latest value of the PPG signal for heart rate visualization
- **g_br_graph**: Latest value of the respiratory signal for visualization

By separating the network operations into their own thread, the system ensures that the RESTful API does not block core processing tasks, maintaining real-time performance. The stateless nature of the RESTful API allows for easy integration with external applications through standardized HTTP communication, providing continuous access to vital sign data without disrupting the ongoing processing within the system.

The HTTP server is initialized in the *MainWindow* constructor by invoking the *startHttpSrvrThread* function, which takes parameters such as the port number, network interface, verbosity level, and URL prefix. The server operates in its own thread, ensuring that network operations remain separate from the main application and do not interfere with real-time processing. **Data transmission** is managed within the *UpdateProcessFrame* function, which is executed every 33 milliseconds to maintain a consistent frame rate of 30 fps. During each cycle, the latest frame and

¹<https://github.com/Corvusoft/restbed>

vital sign values are prepared for transmission. The HTTP server operates in two parallel modes:

1. **Request-Response Mode:** The server listens for incoming HTTP requests via the RESTful API on port 8080 (`/vhealth`). Upon receiving a request, it responds with the latest numerical vital sign data (heart rate, breathing rate, oxygen saturation, and related status flags). Video data is not streamed in this mode.
2. **Continuous Streaming Mode:** Simultaneously, the server continuously streams two video feeds without requiring explicit requests from the client:
 - `http://127.0.10.1:8081/mainstream` – Streams the cropped main camera feed as an MJPEG stream on port 8081.
 - `http://127.0.10.1:8081/pulsestream` – Streams the normalized pulsating face data as an MJPEG stream on port 8081.

In the streaming mode, MJPEG is used for video compression. This format compresses each frame independently, eliminating temporal dependencies, meaning that each frame is compressed and transmitted without needing information from adjacent frames. This approach prevents temporal artifacts and ensures that the loss of one frame does not affect the quality of subsequent frames, making it ideal for real-time streaming with minimal latency and physiological assessment purposes.

Both modes, request-response, and continuous streaming, run concurrently within the HTTP server, supported by asynchronous and non-blocking I/O operations. This enables the server to handle numerical data requests while continuously pushing video streams to connected clients in real time. The separate threading ensures that network operations do not disrupt the core processing pipeline, preserving the real-time performance of the system. This architecture supports multiple simultaneous client connections, allowing for real-time monitoring across various devices. It ensures reliable, low-latency transmission of both video and vital sign data without disrupting ongoing system operations.

5 Performance evaluation of the real-time camera-based rPPG system

This section outlines the experimental methodology and evaluation strategy used to assess the proposed real-time rPPG system. We describe the setup of two system configurations, detail the datasets used, and report both quantitative metrics and processing speed. This structured evaluation enables us to analyze the trade-offs between computational efficiency and physiological signal accuracy across real-time and high-performance environments.

We evaluated the performance of the real-time camera-based rPPG system in two configurations. The first operates without computational constraints, suitable for high-performance computing environments such as cloud servers or workstations, using heavy deep learning models and advanced signal processing algorithms for high-accuracy biosignal extraction. The second configuration is designed for low-power systems and end user equipment, with faster components and algorithmic adjustments to ensure real-time processing and efficient resource usage. Performance metrics and computational efficiency are analyzed to evaluate the balance between accuracy and real-time operation.

5.1 Experimental setup and configurations

The experimental setup for the real-time rPPG prototype consists mainly of two configurations derived from the Face2PPG pipeline [6]: Face2PPG-RT, implemented in C++14 for real-time processing on low-power systems, and Face2PPG-Server, implemented in Python 3.8 for high-accuracy, resource-intensive tasks. The evaluation compares their performance, focusing on computational efficiency and signal accuracy under different operational constraints. Table 1 details the modules and methods across these configurations.

Face2PPG-RT is designed for real-time performance in constrained computational platforms such as embedded systems or mobile devices. This configuration is evaluated in two setups: *Configuration 1* uses the Dlib HOG-based face detector

and basic FFT for frequency analysis. In this FFT-based approach, a 12-second input signal (about 360 samples) is first smoothed using a Hamming window. Then, it is zero-padded to make it five times longer (around 1800 points) before computing the frequency spectrum using the DFT. and *Configuration 2* uses the faster OpenCV YuNet CNN [42] face detector and Welch’s method for spectral analysis to improve signal robustness while preserving real-time processing capabilities; here, a 12-second input signal is processed by dividing it into 256-sample segments with an overlap of 200 samples (approximately 78%), applying a Hamming window to each segment, and averaging the power spectral densities derived from 2048-point FFTs of these segments. Both configurations use the ERT-GTX model [46] in Dlib library (version 19.23) for face alignment, geometric skin segmentation focusing on cheeks and forehead, and FIR filtering with a Lanczos window. The system, compiled using g++ 7.5.0, incorporates a network module, camera capture, and GUI for full operation. However, the evaluation focuses on the core video processing and signal analysis components to ensure an accurate comparison with the server-based setup. The performance of Face2PPG-RT is enhanced by leveraging C/C++ software libraries such as *Lapack* and *BLAS* for efficient linear algebra operations, *OpenMP* for parallelization across multiple processor cores, and *FFTW3* for fast and optimized discrete Fourier transform (DFT) calculations in frequency-domain analysis. These libraries enhance computational efficiency, enabling the system to maintain real-time performance in resource-constrained environments. Face2PPG-Server prioritizes accuracy by using more computationally demanding algorithms. This configuration is tested with two pipelines: *Normalized Pipeline* uses a deep learning-based Single Shot Multibox Detection (SSD) face detector, along with the Deep Alignment Network (DAN) for face alignment [51], and processes the entire normalized facial skin region for signal extraction. *Multiregion Pipeline* also uses SSD and DAN but dynamically selects the optimal skin regions for signal extraction based on quality metrics across multiple facial regions. For spectral analysis, both Face2PPG-Server pipelines use Welch’s method with parameters identical to those described for the Face2PPG-RT Configuration 2

(i.e., 256-sample segments with 200-sample overlap, Hamming windowing, and 2048-point FFTs per segment from a 12-second signal).

Face2PPG-RT was tested on a laptop with an Intel® Core i7-6700HQ CPU (8 cores) with Intel® HD Graphics 530 and 8GB of RAM, running Linux Ubuntu 18.04.6. In contrast, Face2PPG-Server was evaluated on a high-performance workstation equipped with an AMD® Ryzen 3700X 8-core processor, 64GB of RAM, and two NVIDIA GeForce® RTX 2080 GPUs. This system can handle the heavier computational loads required by deep learning modules and complex signal processing tasks. The use of two different hardware platforms is justified by the different goals of each configuration. Face2PPG-RT was tested on mid-range hardware to simulate performance in end-user equipment, while Face2PPG-Server was tested on a high-performance system to evaluate the maximum potential of the algorithms without real-time constraints. This distinction allows for a fair comparison between configurations, highlighting the trade-offs between computational efficiency and accuracy in each operational context.

5.2 Benchmark datasets and Evaluation Metrics

We evaluate the rPPG system implementations using four publicly available datasets: LGI-PPGI [52], COHFACE [53], UBFC-RPPG [54], and PURE [55]. These datasets consist of RGB video recordings under different conditions, with reference physiological data collected using medical-grade fingertip pulse oximeters. This approach allows us to compare the extracted signals with ground truth medical data, ensuring reliable performance validation. While our system is designed for real-time rPPG monitoring using live camera input, we simulate real-time conditions by processing pre-recorded videos, which provides consistent frame capture. In real-time applications, frame capture may not always be as regular, but we have implemented strategies, such as recalculating the frame rate for filtering and FFT [9], to handle irregularities. Rolling shutter effects occur when the camera sensor captures the image line by line, and movement during exposure causes different parts of the image to be captured at slightly different times, resulting in distortion. However, in these datasets and typical rPPG scenarios where

Table 1: Configuration Setups and Modules for Real-time and Cloud-based rPPG Systems.

Module	Face2PPG-RT <i>Config. 1</i>	Face2PPG-RT <i>Config. 2</i>	Face2PPG-Server <i>Normalized</i>	Face2PPG-Server <i>Multiregion</i>
Face Detection	Dlib HOG	OpenCV YuNet	OpenCV SSD	OpenCV SSD
Face Alignment	Dlib ERT GTX	Dlib ERT GTX	DAN	DAN
Face Normalization	Mesh (131 triangles)	Mesh (131 triangles)	Mesh (131 triangles)	Mesh (131 triangles)
Skin Segmentation	Geometrical (Patches)	Geometrical (Patches)	Geometrical (Whole Face)	Geometrical (Best Regions)
RBG to BVP	Lab	Lab	POS	POS
Filtering	FIR BPF (Lanczos win.)	FIR BPF (Lanczos win.)	FIR BPF (Kaiser win.)	FIR BPF (Kaiser win.)
Spectral Analysis	FFT (Hamming win.)	Welch (Hamming win.)	Welch (Hamming win.)	Welch (Hamming win.)
Language	C++	C++	Python	Python

subjects remain steady in front of the camera, notable rolling shutter effects are not expected to significantly impact performance.

COHFACE contains 160 videos of 40 subjects (12 females, 28 males, average age 35.6 years) recorded at 20 Hz and 640x480 resolution using a *Logitech HD C525* webcam. Ground truth heart rate and breathing rate were measured using a fingertip pulse oximeter and respiration belt from *Thought Technology*. Videos were recorded under natural and studio lighting. LGI-PPGI includes 24 videos of 6 subjects (1 female, 5 males) aged 25-42, recorded at 25 Hz and 640x480 resolution using a *Logitech HD C270* webcam. Scenarios include "resting," "rotation," "talking," and "gym," each introducing unique challenges for rPPG extraction. Heart rate was recorded using an FDA-approved *pulox CMS50E* pulse oximeter at 60 Hz. UBFC-RPPG is divided into UBFC1 (8 videos) and UBFC2 (42 videos). UBFC1 captures subjects sitting still, while UBFC2 involves participants performing a mathematical task to induce blood volume pulse variations. Videos were recorded at 30 Hz and 640x480 resolution using a *Logitech C920 HD Pro* webcam. Ground truth heart rate data was captured with a *pulox CMS50E* pulse oximeter at 60 Hz. PURE comprises 60 videos from 10 subjects (8 males, 2 females), recorded at 30 Hz and 640x480 resolution using an *eco274CVGE* camera. Six scenarios involve controlled head movements. Ground truth pulse data was collected with a *pulox CMS50E* pulse oximeter at 60 Hz.

To validate the performance of our system, each video from these datasets was processed. The heart rate estimations generated by our rPPG pipeline, typically over a 12-second sliding window with updates every second (as detailed in Section 3.1), were then temporally synchronized with the reference HR time series provided with each dataset. For each corresponding segment, the estimated HR was compared against the ground-truth HR to compute the evaluation metrics. We use three metrics: Mean Absolute Error (MAE), Root-Mean-Square Error (RMSE), and Pearson Correlation Coefficient (PCC). Since the blood perfusion waveforms differ between facial and fingertip regions [56], we use PCC between heart rate envelopes as a more appropriate metric for evaluating performance, rather than direct waveform comparisons.

5.3 Comparative analysis of real-time and offline rPPG system configurations

In this comparative analysis, we assess the performance of the previously depicted configurations in terms of accuracy in computing heart rate using the datasets introduced in the benchmark subsection. Moreover, we measure the speed performance of each configuration.

5.3.1 Accuracy performance in vital signs measurement

To assess the agreement between the rPPG systems and medical-grade standard PPG systems,

we replicate the experiments conducted in [6]. The evaluation is conducted using the LGI-PPGI database, which includes multiple scenarios that simulate real-world conditions, such as video conferencing, gym environments, and outdoor settings with varying lighting conditions. These scenarios include both static and dynamic head movements. Additionally, we evaluated the system using the COHFACE database, which presents challenges such as heavily compressed videos and uncontrolled lighting with shadows. The UBFC-RPPG database (UBFC1 and UBFC2) is also included, providing high-quality videos recorded under controlled conditions, simulating a medical premises environment. By leveraging these datasets, we aim to evaluate the accuracy of the real-time rPPG system across different operational contexts, reflecting its performance in both controlled and uncontrolled conditions. The results are presented in Table 2. The performance metrics reported in Table 2 (MAE, RMSE, and PCC) were derived by first calculating these values for each individual video sequence within a given dataset. The table presents the mean of these per-video results for RMSE and PCC, and the mean \pm standard deviation for MAE, aggregated per dataset.

The table shows that results from real-time setups are just slightly less effective than those from server setups. Among the server configurations, using multiple regions clearly yields better outcomes. As for real-time setups, we observed that *RT Config. 2*, which utilizes the Welch’s frequency estimation method, performs better than the *RT Config. 1*, coming quite close to the performance of the server setup that uses simple face normalization. These findings show that the impact of the performance of the real-time configuration is relatively minimal, across different conditions.

5.3.2 Speed performance

Table 3 illustrates the speed performance of the different modules within the Face2PPG pipelines across the four proposed configurations. These configurations are divided into two primary categories: User Equipment (targeted for real-time operation) and Cloud (for unconstrained conditions, typically found in server environments).

The outcomes for *RT Config. 1* reveal that the processing time required for each frame is approximately 14.11 milliseconds (ms). The most significant contributor to this processing time is the ‘Face Detection’ module, which consumes 5.48 ms per frame. Despite the demanding computational steps, this configuration achieves an impressive frame rate of 71 frames per second (FPS), ensuring seamless real-time operation. In contrast, the findings for *RT Config. 2* showcase a more optimized performance, with each frame taking only about 9.69 ms to process. Notably, the ‘Face Detection’ time has been substantially reduced in this configuration, clocking in at 1.1 ms, as compared to *RT Config. 1*. Consequently, this acceleration in processing speed elevates the FPS to a commendable 103, further enhancing the system’s real-time capabilities.

In server conditions without real-time constraints, more intensive processing is feasible. This is evident from the *Server-Normalized* configuration, where the total processing time per frame is 116.46 ms, significantly higher than the embedded real-time configurations. Despite the increased processing time, the system maintains a respectable FPS of 8.59. Remarkably, ‘Face Alignment’ contributes substantially to this processing time, requiring up to 82.52 ms. Meanwhile, the *Server-Multiregion* configuration introduces additional processing intricacies, leading to a total frame processing time of 221.87 ms. This nearly doubles the processing time compared to the *Server-Normalized* configuration, resulting in a relatively lower FPS of 4.51. A key observation is the ‘Skin Segmentation’ module, which, in this configuration, demands 105.41 microseconds, underscoring the complexity introduced by multi-region analysis.

Table 3 provides an in-depth exploration of the speed performance of the proposed Face2PPG pipeline across various configurations. While the embedded configurations are tailored for real-time applications, the cloud configurations, designed for server environments, accommodate more intensive data processing and analysis, albeit at a reduced FPS.

6 Conclusion

Current biosignal monitoring systems often exhibit limitations in key areas such as real-time

Table 2: Error comparison between the four different configurations of the proposed rPPG system in four different databases. Two configurations of the real-time system, and two configurations for high performance computers without any constraint.

Pipeline	LGI-PPGI		COHFACE		UBFC1		UBFC2	
	MAE \pm SD	PCC	MAE \pm SD	PCC	MAE \pm SD	PCC	MAE \pm SD	PCC
Face2PPG-Server <i>Normalized</i>	8.7 \pm 8.4	0.50	9.4 \pm 4.8	0.10	1.2 \pm 0.4	0.94	1.4 \pm 1.5	0.95
Face2PPG-Server <i>Multiregion</i>	4.5 \pm 3.3	0.57	8.0 \pm 4.4	0.06	0.9 \pm 0.4	0.96	0.9 \pm 0.9	0.98
Face2PPG-RT <i>Configuration 1</i>	6.4 \pm 6.8	0.45	10.8 \pm 5.5	-0.04	1.4 \pm 0.5	0.80	4.7 \pm 4.6	0.72
Face2PPG-RT <i>Configuration 2</i>	5.9 \pm 8.0	0.49	11.3 \pm 7.3	-0.01	1.5 \pm 1.2	0.83	6.7 \pm 6.1	0.54

Table 3: Performance speed for individual modules in various Face2PPG pipeline configurations, as well as the overall speed per face and frame.

Module	User equipment configurations		Cloud configurations	
	RT Config. 1	RT Config. 2	Server-Normalized	Server-Multiregion
	ms/frame	ms/frame	ms/frame	ms/frame
Face Detection	5.48	1.10	20.35	20.35
Face Alignment	4.48	3.74	82.52	82.52
Face Normalization	3.67	4.37	12.48	12.48
Skin Segmentation	8.23 us	8.23 us	95.57 us	105.41
RBG to BVP	0.462	0.462	0.0798	0.0798
Filtering	1.432 us	1.432 us	0.163 us	0.162 us
Spectral Analysis	5.85 us	5.85 us	1.02	1.02
Total	14.11	9.69	116.46	221.87
Total FPS	71	103	8.59	4.51

data processing, system scalability, and interoperability. To address these challenges, this work focused on the design and implementation of a real-time remote photoplethysmography (rPPG) system capable of non-contact heart rate measurement using RGB cameras, with integrated network capabilities for data transmission via a RESTful API and HTTP streaming. The system includes an event-driven user interface, carefully optimized for resource and energy efficiency. The real-time rPPG system is structured to meet the requirements of both resource-constrained devices and high-performance systems. It follows a modular architecture, comprising distinct components

for sensing, processing, communications, storage, and user interaction. These components were optimized to ensure continuous real-time operation and stable performance, even under conditions such as irregular frame rates and potential frame drops. Key optimizations include efficient algorithms for face detection, alignment, and signal processing, as well as dynamic adjustments in the processing pipeline to maintain accuracy. Additionally, real-time quality metrics, such as head movement tracking, were implemented to assess the reliability of biosignal extraction. These metrics provide feedback to the user to enhance their positioning and environmental conditions,

improving the accuracy and efficiency of the measurements. The system demonstrated effective management of real-time challenges, including frame dropping and reduced frame rates caused by network constraints or low-light conditions. By recalculating frame rates for filtering and frequency-domain analysis, these issues were mitigated without significant accuracy loss. The results suggest that the system can operate effectively with reduced data, up to 16 times less in some scenarios, without substantially compromising rPPG measurement accuracy [9]. This supports the potential for improved energy efficiency and reduced power consumption, especially in embedded applications. These findings are consistent with studies such as Mohan et al. (2018), which showed that performance in object tracking could be maintained with significantly lower frame rates when appropriate strategies are applied [57]. Moreover, the real-time rPPG system achieved comparable performance to offline, server-based systems while operating at speeds up to 20 times faster. This efficiency was maintained without significant degradation in the accuracy of heart rate measurements. The system’s ability to function at high frame rates, even with reduced resolution and sampling rates, highlights its potential for deployment in devices with limited computational power, such as mobile or embedded systems. We evaluated the accuracy using four publicly available datasets, which include varying environmental conditions such as low light, low dynamic range with strong backlighting, and highly compressed videos. These tests allowed us to assess the robustness under real-world conditions.

Beyond its direct applications, this work offers specific value for other researchers. The system implementation in C++, with minimal third-party dependencies, differs from many rPPG prototypes typically developed for offline analysis or in Python, and has been designed for deployment on low-power embedded platforms. Its modular and concurrent architecture facilitates adaptation for different experimental setups or integration into more complex clinical interfaces, allowing researchers to build upon a stable real-time foundation. The design and C++ implementation, optimized for efficiency on low-power platforms with minimal dependencies, thus constitute a practical resource for the research community. Furthermore, the technical design of the

system provides a reference for real-time biomedical signal processing, particularly in addressing challenges related to scheduling, concurrency, and latency under operational constraints. The analysis of these engineering aspects reveals important trade-offs between system responsiveness, computational load, and the fidelity of physiological signals. These insights are also relevant to fields such as embedded systems, robotics, and hybrid intelligence, contributing to the broader development of more robust and efficient context-aware computing systems.

Our contributions aim to solidify rPPG as a viable and versatile tool within modern healthcare and human-computer interaction, offering insights into the creation and design of more reliable and accurate real-time rPPG systems. Future work will focus on further optimizing the system for a range of deployment scenarios, including increasing robustness under variable network and hardware conditions, as well as expanding its applicability in distributed healthcare environments.

Acknowledgements. The research was supported by University of Oulu, the 6G Flagship (369116), Profi5 HiDyn programme (326291), and Profi7 Hybrid intelligence program (352788), funded by the Research Council of Finland, and the Orion Research Foundation (Grant: Apurahat Constantino Álvarez Casado).

Declarations

Funding

The research was supported by University of Oulu, the 6G Flagship (369116), Profi5 HiDyn programme (326291), and Profi7 Hybrid intelligence program (352788), funded by the Research Council of Finland, and the Orion Research Foundation (Grant: Apurahat Constantino Álvarez Casado).

Conflict of interest/Competing interests

The authors declare that they have no conflict of interest.

Ethics approval and consent to participate

Not applicable

Consent for publication

Not applicable

Availability of data and materials

The datasets analyzed during the current study are publicly available and detailed in Section 5.2. No new datasets were generated. The source code for the system described in this article is available on GitHub at <https://github.com/Arritmic/rt-rppg>.

Author Contributions

Constantino Álvarez Casado: Writing – review & editing, Writing – original draft, Visualization, Validation, Software, Methodology, Investigation, Formal analysis, Conceptualization. Sasan Sharifpour: Writing – review & editing, Methodology, Investigation, Software. Manuel Lage Cañellas: Writing – review & editing, Software, Methodology, Investigation. Nhi Nguyen: Writing – review & editing, Validation, Software, Investigation. Le Nguyen: Writing – review & editing, Validation, Methodology, Investigation, Formal analysis. Miguel Bordallo López: Writing – review & editing, Writing – original draft, Visualization, Validation, Supervision, Software, Methodology, Investigation, Formal analysis, Conceptualization, Funding acquisition.

All authors reviewed the manuscript.

References

- [1] Taylor, J.K., Ahmed, F.Z.: Clinical pathways guided by remotely monitoring cardiac device data: The future of device heart failure management? *Arrhythmia & Electrophysiology Review* **12** (2023)
- [2] Dunn, J., Coravos, A., Fanarjian, M., Ginsburg, G.S., Steinhubl, S.R.: Remote digital health technologies for improving the care of people with respiratory disorders. *The Lancet Digital Health* **6**(4), 291–298 (2024)
- [3] Huang, B., Hu, S., Liu, Z., Lin, C.-L., Su, J., Zhao, C., Wang, L., Wang, W.: Challenges and prospects of visual contactless physiological monitoring in clinical study. *NPJ Digital Medicine* **6**(1), 231 (2023)
- [4] Albahri, O.S., Albahri, A.S., Mohammed, K., Zaidan, A., Zaidan, B., Hashim, M., Salman, O.H.: Systematic review of real-time remote health monitoring system in triage and priority-based sensor technology: Taxonomy, open challenges, motivation and recommendations. *Journal of medical systems* **42**, 1–27 (2018)
- [5] Malasinghe, L.P., Ramzan, N., Dahal, K.: Remote patient monitoring: a comprehensive study. *Journal of Ambient Intelligence and Humanized Computing* **10**, 57–76 (2019)
- [6] Álvarez Casado, C., Bordallo López, M.: Face2ppg: An unsupervised pipeline for blood volume pulse extraction from faces. *IEEE Journal of Biomedical and Health Informatics* **27**(11), 5530–5541 (2023) <https://doi.org/10.1109/JBHI.2023.3307942>
- [7] Antolinos, E., García-Rial, F., Hernández, C., Montesano, D., Godino-Llorente, J.I., Grajal, J.: Cardiopulmonary activity monitoring using millimeter wave radars. *Remote Sensing* **12**(14), 2265 (2020)
- [8] Dasari, A., Prakash, S.K.A., Jeni, L.A., Tucker, C.S.: Evaluation of biases in remote photoplethysmography methods. *NPJ digital medicine* **4**(1), 91 (2021)
- [9] Nguyen, N., Nguyen, L., Li, H., Bordallo López, M., Álvarez Casado, C.: Evaluation of video-based rppg in challenging environments: Artifact mitigation and network resilience. *Computers in Biology and Medicine* **179**, 108873 (2024) <https://doi.org/10.1016/j.compbiomed.2024.108873>
- [10] Ackerman, M.J., Filart, R., Burgess, L.P., Lee, I., Poropatich, R.K.: Developing next-generation telehealth tools and technologies: patients, systems, and data perspectives. *Telemedicine and e-Health* **16**(1), 93–95 (2010)

- [11] Jiang, T., Sun, Z., Fu, S., Lv, Y.: Human-ai interaction research agenda: A user-centered perspective. *Data and Information Management* **8**(4), 100078 (2024)
- [12] Buttazzo, G.: Research trends in real-time computing for embedded systems. *ACM SIGBED Review* **3**(3), 1–10 (2006)
- [13] Lin, Y.-C., Lin, Y.-H.: A study of color illumination effect on the snr of rppg signals. In: 2017 39th Annual International Conference of the IEEE Engineering in Medicine and Biology Society (EMBC), pp. 4301–4304 (2017). <https://doi.org/10.1109/EMBC.2017.8037807>
- [14] Song, R., Zhang, S., Cheng, J., Li, C., Chen, X.: New insights on super-high resolution for video-based heart rate estimation with a semi-blind source separation method. *Computers in biology and medicine* **116**, 103535 (2020)
- [15] Setchfield, K., Gorman, A., Simpson, A.H.R., Somekh, M.G., Wright, A.J.: Effect of skin color on optical properties and the implications for medical optical technologies: a review. *Journal of Biomedical Optics* **29**(1), 010901–010901 (2024) <https://doi.org/10.1117/1.JBO.29.1.010901>
- [16] Kumar, M., Veeraraghavan, A., Sabharwal, A.: Distanceppg: Robust non-contact vital signs monitoring using a camera. *Biomedical optics express* **6**(5), 1565–1588 (2015)
- [17] Narayanan, A., Zhang, X., Zhu, R., Hassan, A., Jin, S., Zhu, X., Zhang, X., Rybkin, D., Yang, Z., Mao, Z.M., Qian, F., Zhang, Z.-L.: A variegated look at 5g in the wild: Performance, power, and qoe implications. In: Proceedings of the 2021 ACM SIGCOMM 2021 Conference. SIGCOMM '21, pp. 610–625. Association for Computing Machinery, New York, NY, USA (2021). <https://doi.org/10.1145/3452296.3472923> . <https://doi.org/10.1145/3452296.3472923>
- [18] Kim, J.S., Kim, M.-G., Pan, S.B.: A study on implementation of real-time intelligent video surveillance system based on embedded module. *EURASIP Journal on Image and Video Processing* **2021**(1), 35 (2021)
- [19] Zhao, L.-l., Jiang, X.-l., Li, L.-m., Zeng, G.-q., Liu, H.-j.: Optimization of a robust collaborative-relay beamforming design for simultaneous wireless information and power transfer. *Frontiers of Information Technology & Electronic Engineering* **19**(11), 1432–1443 (2018) <https://doi.org/10.1631/FITEE.1601268>
- [20] McDuff, D.J., Blackford, E.B., Estepp, J.R.: The impact of video compression on remote cardiac pulse measurement using imaging photoplethysmography. In: 2017 12th IEEE International Conference on Automatic Face & Gesture Recognition (FG 2017), pp. 63–70 (2017). <https://doi.org/10.1109/FG.2017.17>
- [21] Blackford, E., Estepp, J.: Effects of frame rate and image resolution on pulse rate measured using multiple camera imaging photoplethysmography. *Progress in Biomedical Optics and Imaging - Proceedings of SPIE* **9417** (2015) <https://doi.org/10.1117/12.2083940>
- [22] Hanfland, S., Paul, M.: Video format dependency of ppgi signals. In: Proceedings of the International Conference on Electrical Engineering, vol. 1, p. 2 (2016). http://radio.feld.cvut.cz/conf/poster/poster2016/proceedings/Section_BI/BI.007_Hanfland.pdf
- [23] Zhao, C., Lin, C.-L., Chen, W., Li, Z.: A novel framework for remote photoplethysmography pulse extraction on compressed videos. In: 2018 IEEE/CVF Conference on Computer Vision and Pattern Recognition Workshops (CVPRW), pp. 1380–138009 (2018). <https://doi.org/10.1109/CVPRW.2018.00177>
- [24] Botina-Monsalve, D., Benezeth, Y., Miteran, J.: Rtrppg: An ultra light 3dcnn for real-time remote photoplethysmography. In: 2022 IEEE/CVF Conference on Computer Vision and Pattern Recognition Workshops (CVPRW), pp. 2145–2153 (2022). <https://doi.org/10.1109/CVPRW56347.2022.00233>

- [25] Hasan, Z., Dey, E., Ramamurthy, S.R., Roy, N., Misra, A.: RhythmEdge: Enabling contactless heart rate estimation on the edge. In: IEEE International Conference on Smart Computing (2022)
- [26] Reuther, A., Michaleas, P., Jones, M., Gadeppally, V., Samsi, S., Kepner, J.: Ai accelerator survey and trends. In: 2021 IEEE High Performance Extreme Computing Conference (HPEC), pp. 1–9 (2021). IEEE
- [27] Zhou, C., Liu, M., Qiu, S., Cao, X., Fu, Y., He, Y., Jiao, H.: Sagitta: An energy-efficient sparse 3d-cnn accelerator for real-time 3d understanding. IEEE Internet of Things Journal (2023)
- [28] Li, W., Liewig, M.: A survey of ai accelerators for edge environment. In: Trends and Innovations in Information Systems and Technologies: Volume 2 8, pp. 35–44 (2020). Springer
- [29] Czarnul, P., Proficz, J., Drypczewski, K.: Survey of methodologies, approaches, and challenges in parallel programming using high-performance computing systems. Scientific Programming **2020**(1), 4176794 (2020)
- [30] Kopetz, H., Steiner, W.: Real-Time Systems, 3rd edn., p. 406. Springer, ??? (2022). <https://doi.org/10.1007/978-3-031-11992-7> . eBook published on 22 September 2022, hardcover published on 24 September 2022, softcover published on 25 September 2023
- [31] Salehian, S., Liu, J., Yan, Y.: Comparison of threading programming models. In: 2017 IEEE International Parallel and Distributed Processing Symposium Workshops (IPDPSW), pp. 766–774 (2017). IEEE
- [32] Buono, D.: Optimizations and cost models for multi-core architectures: an approach based on parallel paradigms. PhD thesis, University of Pisa, Italy (2014)
- [33] Berjón, D., Arnaldo, S., Morán, F.: A parallel implementation of 3D Zernike moment analysis. In: Owens, J.D., Lin, I.-J., Zhang, Y.-J., Beretta, G.B. (eds.) Parallel Processing for Imaging Applications, vol. 7872, p. 787209. SPIE, ??? (2011). <https://doi.org/10.1117/12.876683> . International Society for Optics and Photonics. <https://doi.org/10.1117/12.876683>
- [34] Buttazzo, G.: Hard Real-Time Computing Systems, 4th edn., p. 492. Springer, ??? (2023). <https://doi.org/10.1007/978-3-031-45410-3> . eBook published on 15 December 2023, hardcover published on 16 December 2023, softcover due on 29 December 2024
- [35] Lorenzon, A.F., Sartor, A.L., Cera, M.C., Beck, A.C.S.: Optimized use of parallel programming interfaces in multithreaded embedded architectures. In: 2015 IEEE Computer Society Annual Symposium on VLSI, pp. 410–415 (2015). IEEE
- [36] Vanneschi, M.: High Performance Computing. Parallel Processing Models and Architectures. Pisa University Press, ??? (2014). <https://books.google.fi/books?id=yTuToAEACAAJ>
- [37] Leidi, T., Heeb, T., Colla, M., Thiran, J.-P.: Event-driven scheduling for parallel stream processing. In: 2011 Sixth International Symposium on Parallel Computing in Electrical Engineering, pp. 36–41 (2011). IEEE
- [38] Díez, D.B.: Parallel computer vision algorithms for graphics processing units. PhD thesis, Universidad Politécnica de Madrid (2016)
- [39] Bradski, G.: The opencv library. Dr. Dobb’s Journal: Software Tools for the Professional Programmer **25**(11), 120–123 (2000)
- [40] King, D.E.: Dlib-ml: A machine learning toolkit. The Journal of Machine Learning Research **10**, 1755–1758 (2009)
- [41] Lazar, G., Penea, R.: Mastering Qt 5: Create Stunning Cross-platform Applications Using C++ with Qt Widgets and QML with Qt Quick. Packt Publishing Ltd, ??? (2018)
- [42] Wu, W., Peng, H., Yu, S.: Yunet: A tiny

- millisecond-level face detector. *Machine Intelligence Research*, 1–10 (2023) <https://doi.org/10.1007/s11633-023-1423-y>
- [43] Howard, A.G., Zhu, M., Chen, B., Kalenichenko, D., Wang, W., Weyand, T., Andreetto, M., Adam, H.: Mobilenets: Efficient convolutional neural networks for mobile vision applications. *arXiv preprint arXiv:1704.04861* (2017)
 - [44] King, D.E.: Dlib-ml: A machine learning toolkit. *Journal of Machine Learning Research* **10**, 1755–1758 (2009)
 - [45] Dalal, N., Triggs, B.: Histograms of oriented gradients for human detection. In: 2005 IEEE Computer Society Conference on Computer Vision and Pattern Recognition (CVPR’05), vol. 1, pp. 886–8931 (2005). <https://doi.org/10.1109/CVPR.2005.177>
 - [46] Álvarez Casado, C., Bordallo López, M.: Real-time face alignment: evaluation methods, training strategies and implementation optimization. *Journal of Real-Time Image Processing*, 1–29 (2021)
 - [47] Nanni, L., Loreggia, A., Lumini, A., Dorizza, A.: A standardized approach for skin detection: Analysis of the literature and case studies. *Journal of Imaging* **9**(2), 35 (2023)
 - [48] Yang, Y., Liu, C., Yu, H., Shao, D., Tsow, F., Tao, N.: Motion robust remote photoplethysmography in cielab color space. *Journal of Biomedical Optics* **21**, 117001 (2016) <https://doi.org/10.1117/1.JBO.21.11.117001>
 - [49] Álvarez Casado, C., Räsänen, P., Nguyen, L.N., Lämsä, A., Peltola, J., Bordallo López, M.: A distributed framework for remote multimodal biosignal acquisition and analysis. In: *Nordic Conference on Digital Health and Wireless Solutions*, pp. 127–146 (2024). Springer
 - [50] De Giovanni, E., Montagna, F., Denking, B.W., Machetti, S., Peón-Quirós, M., Benatti, S., Rossi, D., Benini, L., Atienza, D.: Modular design and optimization of biomedical applications for ultralow power heterogeneous platforms. *IEEE Transactions on Computer-Aided Design of Integrated Circuits and Systems* **39**(11), 3821–3832 (2020)
 - [51] Kowalski, M., Naruniec, J., Trzcinski, T.: Deep alignment network: A convolutional neural network for robust face alignment. In: *Proceedings of the IEEE Conference on Computer Vision and Pattern Recognition Workshops*, pp. 88–97 (2017)
 - [52] Pilz, C.S., Zaunseder, S., Krajewski, J., Blazek, V.: Local group invariance for heart rate estimation from face videos in the wild. In: *2018 IEEE/CVF Conference on Computer Vision and Pattern Recognition Workshops (CVPRW)*, pp. 1335–13358 (2018). <https://doi.org/10.1109/CVPRW.2018.00172>
 - [53] Heusch, G., Anjos, A., Marcel, S.: A reproducible study on remote heart rate measurement. *arXiv preprint arXiv:1709.00962* (2017)
 - [54] Bobbia, S., Macwan, R., Benezeth, Y., Mansouri, A., Dubois, J.: Unsupervised skin tissue segmentation for remote photoplethysmography. *Pattern Recognition Letters* **124**, 82–90 (2019)
 - [55] Stricker, R., Müller, S., Gross, H.-M.: Non-contact video-based pulse rate measurement on a mobile service robot. In: *IEEE Int. Symp. on Robot and Human Interactive Communication*, pp. 1056–62 (2014). <https://doi.org/10.1109/ROMAN.2014.6926392>
 - [56] Allen, J., Murray, A.: Effects of filtering on multisite photoplethysmography pulse waveform characteristics. In: *IEEE Computers in Cardiology*, pp. 485–488 (2004). <https://doi.org/10.1109/CIC.2004.1442980>
 - [57] Mohan, A., Kaseb, A.S., Gauen, K.W., Lu, Y.-H., Reibman, A.R., Hacker, T.J.: Determining the necessary frame rate of video data for object tracking under accuracy constraints. In: *2018 IEEE Conference on Multimedia Information Processing and Retrieval (MIPR)*, pp. 368–371 (2018). <https://doi.org/10.1109/MIPR.2018.8444444>

[org/10.1109/MIPR.2018.00081](https://doi.org/10.1109/MIPR.2018.00081)